Effect of TiO_2 on Thermal and Adhesive Characteristics of Poly(imide siloxane)/TiO_2 Hybrid Films

Cheng-Jung Ko,[1,2] I-Hsiang Tseng,[1] Wha-Tzong Whang,[2] Mei-Hui Tsai[1]

[1]*Department of Chemical and Materials Engineering, National Chin-Yi University of Technology, Taichung 411, Taiwan*
[2]*Department of Materials Science and Engineering, National Chiao Tung University, Hsin-Chu 300, Taiwan*

Received 20 January 2011; accepted 8 April 2011
DOI 10.1002/app.34649
Published online 25 October 2011 in Wiley Online Library (wileyonlinelibrary.com).

ABSTRACT: A novel poly(imide siloxane)/titania (PIS/TiO_2) hybrid film was fabricated by sol-gel process via *in situ* formation of TiO_2 within PIS matrix. Poly(amic acid siloxane) (PAAS) was prepared from 4,4′-oxydiphthalic anhydride, 2,2-bis [4-(4-aminophenoxy) phenyl] propane, and α,ω-bis(3-aminopropyl)polydimethylsiloxane (APPS). Chelating agent, acetylacetone, and catalyst-free polymerization were used to reduce the rate of hydrolysis of titanium alkoxide in the PAAS. X-ray photoelectron spectroscopy data showed that the presence of APPS promotes the Ti surface composition of PIS/TiO_2 hybrid film. The effects of TiO_2 and APPS contents on the characteristics of surface, thermostability, coefficient of thermal expansion (CTE), and the strength of adhesion were investigated. The presence of TiO_2 on the surface of the hybrid films enhanced the adhesive strength at the interface of PIS/TiO_2 hybrid film and copper foil. When more TiO_2 was incorporated into the PIS matrix, the PIS/TiO_2 hybrid film exhibited lower CTE while retaining favorable mechanical and thermal properties. © 2011 Wiley Periodicals, Inc. J Appl Polym Sci 124: 1929–1937, 2012

Key words: poly(imide siloxane); TiO_2; X-ray photoelectron spectroscopy; adhesion; copper foil

INTRODUCTION

Organic/inorganic hybrid materials with unique electrical, magnetic, mechanical, and adhesive properties[1] are produced and studied extensively in the field of material science. Polyimides (PIs) are thermally stable polymers with excellent mechanical properties and low dielectric constants. PIs are used in flexible printed circuits and become some of the most extensively used polymers in semiconductor integrated circuit packaging.[2–7] They are typically modified with siloxane segments to confer low moisture absorption and strong adhesion at the polyimide/substrate interface. Siloxane is known as a release agent due to its low surface energy[8,9] and is possible to enhance the adhesion strength between poly(imide siloxane) (PIS) and alloy[9] or copper foil[10] systems. Two or more layers of PI as well as a thin layer of metals, such as Cr and Ta, are commonly precoated to strengthen the adhesion at the interface of PI and copper.[11–17] The strength of adhesion between PI (or PIS) and copper foil can be increased by incorporating siloxane segments into PI matrix or by adding tantalum ethoxide ($Ta(OEt)_5$) to the PIS matrix.[18–21]

In this study, titanium alkoxide was incorporated into the PIS matrix to reduce the thermal expansion and enhance the adhesion strength between PIS and copper. Nanosized titanium oxide was formed *in situ* using acetylacetone (acac) as a chelating agent to stabilize titanium ethoxide ($Ti(OEt)_4$) in poly(amic acid siloxane) (PAAS). No acid catalyst or water was added to the PAAS/ $Ti(OEt)_4$ solution. The goal of this work was to investigate the surface compositions of Si and Ti on the prepared PIS/TiO_2 hybrid films as well as the influences of the surface content on thermal and mechanical properties. The characterization results from X-ray photoelectron spectroscopy (XPS), thermogravimetric analysis (TGA), thermal mechanical analysis (TMA), and adhesive strength test of a series of PIS/TiO_2 hybrid films were correlated with their constituents.

EXPERIMENTAL

Materials

High-purity octamethylcycloterasiloxane (D4), and 1,3-bis(3-aminopropyl) tetramethyldisiloxane (DSX) were obtained from Tokyo Chemical Industry (TCI). Tetramethylammonium hydroxide pentahydrate (TMAHP, 98%) was acquired from Lancaster. 4,4′-

Correspondence to: M.-H. Tsai (tsaimh@ncut.edu.tw).
Contract grant sponsor: Ministry of Economic Affairs, Republic of China (Taiwan); contract grant number: 98-EC-17-A-07-S1-120

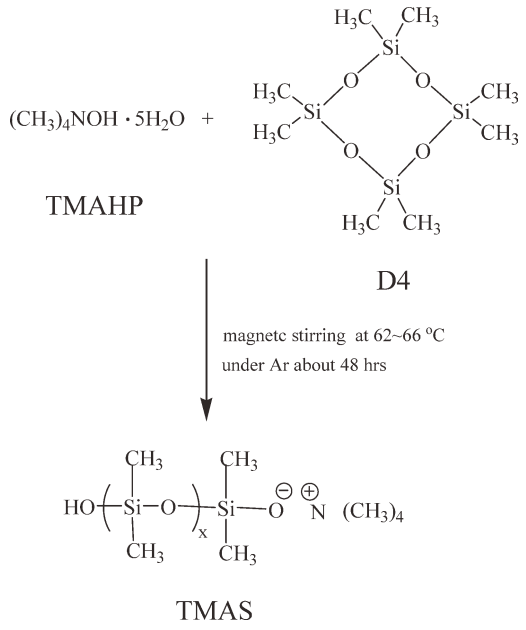

Scheme 1 Synthesis of the catalyst, tetramethylammonium siloxanolate (TMAS).

oxydiphthalic anhydride (ODPA, 98%, Chriskev) was dried in a vacuum oven at 85°C overnight and 2,2-bis[4-(4-aminophenoxy)phenyl]propane (*p*-BAPP, 98%, Aldrich) was dried at 85°C for 8 h before use. $Ti(OEt)_4$ (TCI), acac (TCI), and *N*,*N*-dimethyl formamide (DMF, Tedia) were used as received in the reaction.

Synthesis of α,ω-bis(3-aminopropyl) polydimethylsiloxane oligomer

The catalyst, tetramethylammonium siloxanolate (TMAS), was first synthesized by reacting stoichiometric amounts of TMAHP and D4 with stirring at 60°C under Ar atmosphere for 48 h. Scheme 1 displayed the reaction. The α,ω-bis(3-aminopropyl)polydimethylsiloxane (APPS) oligomer was then prepared from the stoichiometric mixture of DSX and D4 with the addition of 1.0 wt % of TMAS by stirring for 48 h at 80°C under N_2. Continued stirring at 150°C for 3 h under N_2 was followed to decompose the catalyst TMAS. After cooling to room temperature, the above

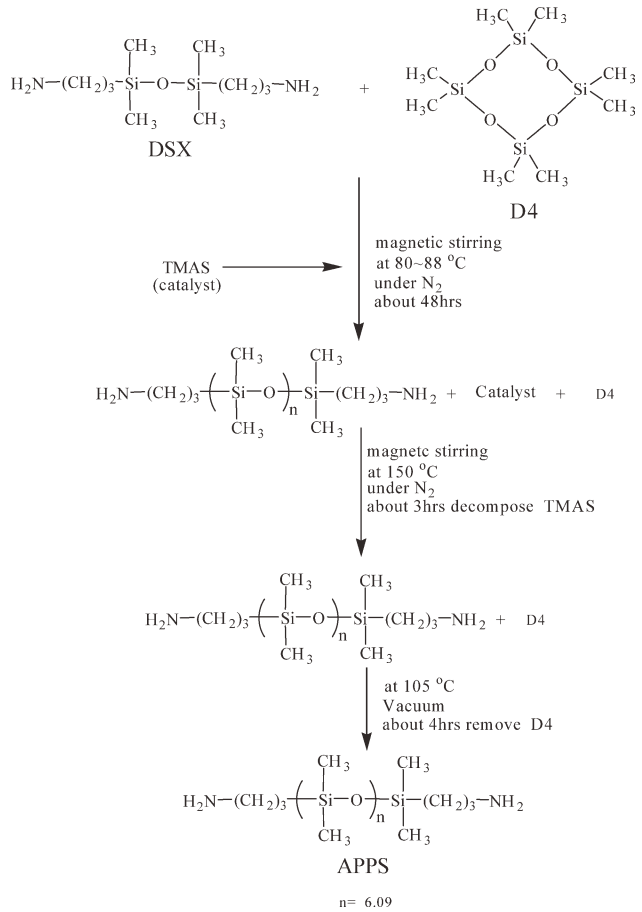

Scheme 2 Synthesis of α, ω-bis (3-aminopropyl) polydimethylsiloxane (APPS) oligomer.

solution was heated again at 105°C for 4 h under vacuum to remove the residual D4.[8,9,22] Scheme 2 presented the reaction of APPS oligomer. APPS with the number average molecular weight of 625 g mol^{-1} was determined by the proton nuclear magnetic resonance (NMR) spectroscopy, which was presented in Table I.

Synthesis of poly(imide siloxane)/titania

PAAS solutions were synthesized by stir mixing stoichiometric amounts of *p*-BAPP, APPS, and ODPA with suitable amount of DMF at room

TABLE I
NMR Chemical Shift of 625 g mol^{-1} APPS

Structures	Hydrogen of the molecule	Integral data	Chemical shift (ppm)
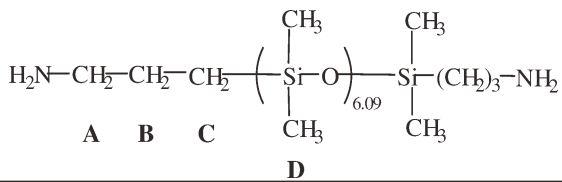	A	0.67	2.60–2.65, a triplet
	B	0.76	1.39–1.44, a doublet and a triplet
	C	0.73	0.46–0.52, a triplet
	D	7.13	0.00–0.05, a multiplet

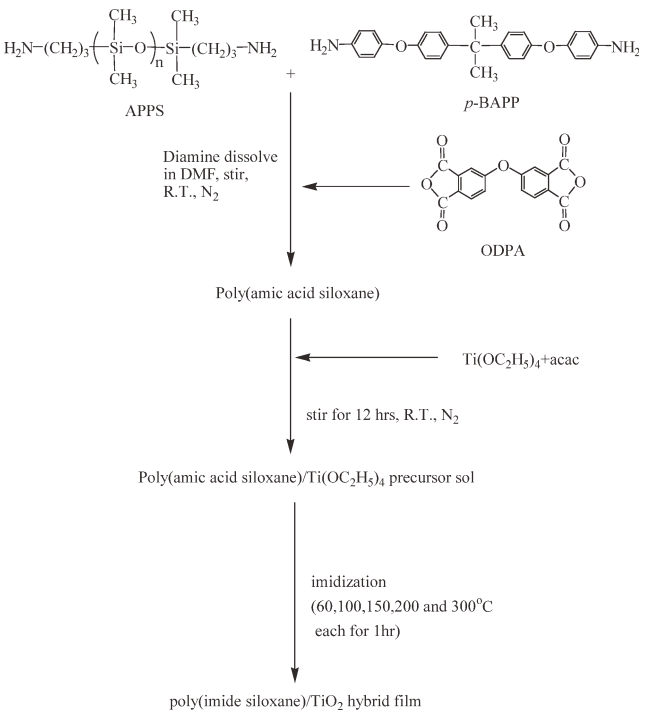

Scheme 3 Synthesis of PIS/TiO_2 hybrid film.

temperature (R.T.) for 2 h under N_2. The precursor sol, PAAS/$Ti(OC_2H_5)_4$ solutions were prepared by adding the mixture with a fixed molar ratio, $Ti(OEt)_4$ to acac, of one-fourth to the above PAAS solution and stirring at R.T. for 12 h under N_2. The chelating agent (acac) was utilized to control the sol-gel reactivity of titanium alkoxides. The metal oxide concentration was expected to be about 1 to 8 wt % within the PIS matrix based on the assumptions of complete imidization, complete conversion of $Ti(OEt)_4$ to TiO_2, and absence of any residual solvent. Scheme 3 presented the reaction.

The PAAS/$Ti(OC_2H_5)_4$ solution was coated on a dust-free glass plate using a doctor blade with a thickness of 650 μm. The gel film was then heated at 60, 100, 200, and 300°C, respectively, each for 1 h to obtain PIS/TiO_2 hybrid films with a thickness ranging from 65 to 75 μm. The PIS/TiO_2 hybrid films were labeled as PIS*x*-*y*-*z*T, where *x*, *y*, and *z* referred to the number average molecular weight of APPS (e.g., $x = 6$ as 625 g mol^{-1}), the weight percentage of APPS and the ideal weight percentage of TiO_2 in PIS/TiO_2 hybrid films, respectively. For example, a label with $y = 0$ or $z = 0$ indicated no addition of APPS or absence of TiO_2 in the hybrid film.

Characterization

Fourier transform infrared (FTIR) absorption spectra of prepared films were recorded between 4000 cm^{-1} and 400 cm^{-1} using a Nicolet Protégé460 spectrometer. TGA was performed using TGA-Q500 (TA Instruments) in the temperature range from 60 to 800°C with a heating rate of 20°C min^{-1} under N_2. The in-plane thermal expansion measurement was used from 50 to 350°C with a heating rate of 5°C min^{-1} using a Du Pont 2940 probe providing 0.05 N in tension to the film. The coefficient of thermal expansion (CTE) between 55 and 200°C was determined. XPS was performed using a PHI Quantera SXM spectrometer with Al Kα radiation source and a pass-energy of 280 eV under constant energy mode. XPS analysis was conducted at R.T. and under the pressure below 10^{-8} torr. The take-off angle used in XPS depth profiling was 45°, and the sputtering rate was 3.97 nm min^{-1}. The adhesion strength tests of PIS or PIS/TiO_2 hybrid films were carried out in accordance to the 180° peel test method (Model HT-8116 Hung TA) with a peel rate of 50.8 mm min^{-1}. Each sample was adhered to a preheated Cu foil substrate at 360°C and under the pressure of 50 kg cm^{-2} for 5 min. The peel strength listed in Table IV was an average of at least four-time measurements on each sample. The dynamic mechanical analysis (DMA) was carried out by means of a thermal analyzer (DMA-2980, TA Instruments) from 60 to 300°C, at a frequency of 1 Hz and heating rate of 3°C min^{-1}.

RESULTS AND DISCUSSION

FTIR

The chemical structure of PIS hybrid films was characterized by FTIR. Figure 1 presented the IR spectra of standard TiO_2, PIS6-10-0T, and PIS6-10-5T. The two hybrid films, with or without TiO_2, showed peaks at 1778 and 1720 cm^{-1}, which were assigned to asymmetrical and symmetrical carbonyl stretching

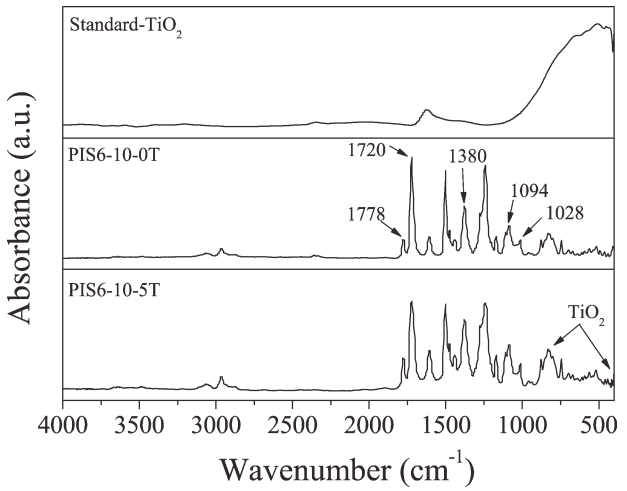

Figure 1 FTIR spectra of standard TiO_2 and the hybrid films, PIS6-10-0T, and PIS6-10-5T. The weight percentage of TiO_2 in hybrid films is 0 and 5 wt %, respectively.

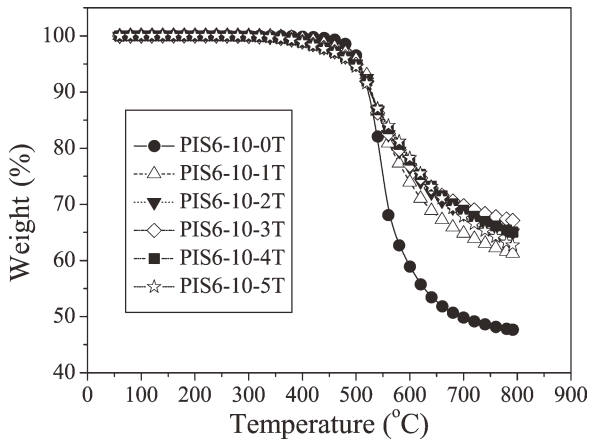

Figure 2 Thermogravimetric profiles of the hybrid films, PIS6-10-*z*T, with various contents of TiO_2. The letter *z* indicates the weight percentage of TiO_2 in hybrid films.

of imide rings, as well as another peak at 1380 cm^{-1}, which was from C—N stretching.[23] The absorption bands at 1028 and 1094 cm^{-1} corresponding to the Si—O—Si stretching of the APPS were observed for both PIS hybrid films. However, TiO_2 stretching bands[1,25,24–26] in the range of 400 to 850 cm^{-1} cannot be distinguished in hybrid films.

TGA

Figures 2 and 3 showed the TGA results of the hybrid films with various TiO_2 contents and the corresponding decomposition temperature (T_d) at 5% weight loss of each sample was listed in Table II. All of the PIS*x*-*y*-*z*T films began to decompose at the temperature around 400°C and had T_d between 495 and 508°C indicating high thermal durability. The value of T_d slightly decreased with the increase of

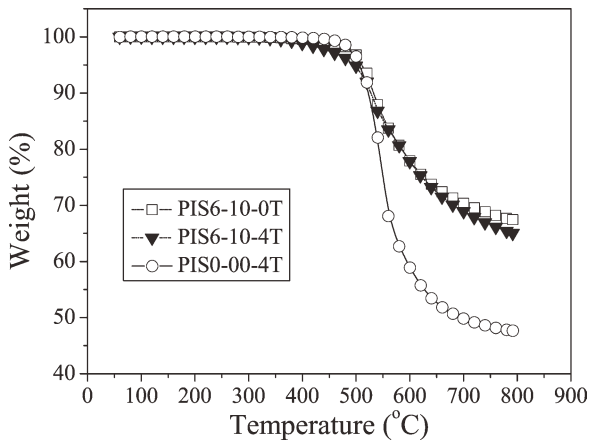

Figure 3 Effect of APPS and TiO_2 on the thermogravimetric profile of PIS*x*-*y*-*z*T hybrid films. The letter *x* indicates the average molecular weight of APPS (e.g. $x = 6$ as 625 g mol^{-1}) and the letter *y* indicates the weight percentage of APPS. The letter *z* indicates the weight percentage of TiO_2 in hybrid films.

TABLE II
Thermal Property of PIS Hybrid Films

Samples	T_d (°C)[1]	CTE (ppm/°C)[2]
PIS6-10-0T	508.4	157.9
PIS6-10-1T	507.7	91.6
PIS6-10-2T	500.6	83.7
PIS6-10-3T	498.9	82.3
PIS6-10-4T	498.3	80.3
PIS6-10-5T	494.8	75.7
PIS0-00-4T	512.4	77.9

[1] Determined by TGA data as the temperature at which 5% weight loss occurs.
[2] Determined by TMA data as the dimension change in the temperature range from 55 to 200°C.

TiO_2 content in films. The presence of TiO_2 may catalytically degrade polyimide matrix that the reduction in thermal stability was observed.[27–29] Figure 2 also revealed that adding TiO_2 improved the char yield. With the presence of 1 wt % TiO_2 in hybrid film, i.e., PIS6-10-1T, the char yield significantly increased to 62% comparing to 50% for PIS6-10-0T.

Determination of coefficients of thermal expansion

Figure 4 showed the TMA results of a series of PIS6-10-*z*T hybrid films. The extent of reduction in dimension change of PIS/TiO_2 hybrid films significantly increased especially when the temperature was higher than 200°C. The CTEs of PIS and PIS/TiO_2 hybrid films were calculated by the dimension change between 55 and 200°C. The obtained CTEs were listed in Table II and plotted in Figure 5 as a function of TiO_2 content. The CTE of all PIS/TiO_2 hybrid films was ~ 50% lower than that of PIS6-10-0T, which contains no TiO_2. It is believed that the linear PIS chains may penetrate into Ti—O—Ti forming semi-IPN crosslink structures in the synthesized

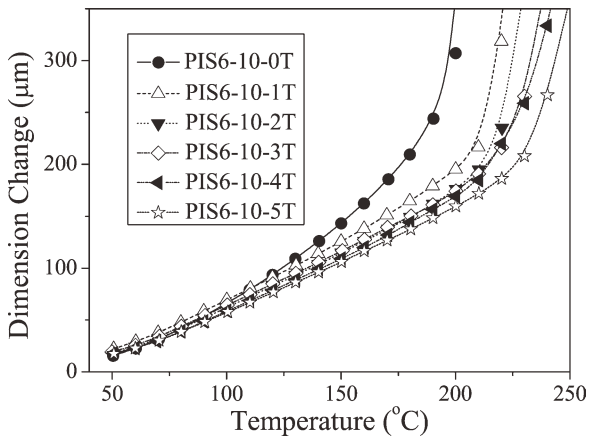

Figure 4 Effect of TiO_2 contents on thermal expansion of the hybrid films, PIS6-10-*z*T. The letter *z* indicates the weight percentage of TiO_2 in hybrid films.

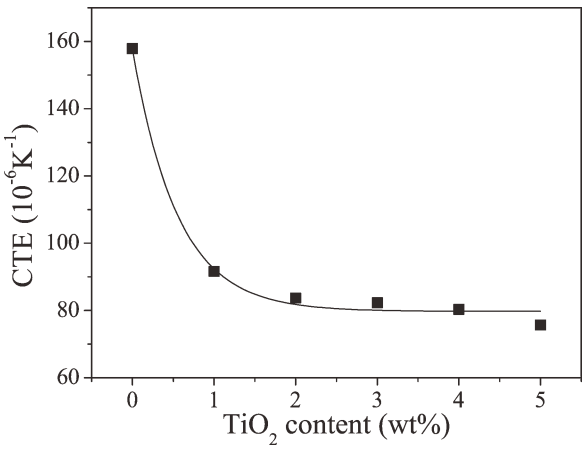

Figure 5 Effect of TiO_2 content on the coefficient of thermal expansion (CTE) of the hybrid films, PIS6-10-*z*T. The letter z indicates the weight percentage of TiO_2 in hybrid films.

hybrid films. Consequently, this stiff 3D-TiO_2 structure was responsible to the limitation of the movement of the linear PIS chains and the reduction of the CTE values of hybrid films. The reliability of adhesion between obtained hybrid films and copper system will be enhanced and the delamination will be prevented in future applications.

XPS

XPS analysis with depth profiling was used to characterize the film surface at various depths. As shown in Table III, the composition of Si (2p) was zero for PIS0-00-4T under depth profiling (30 ~ 120 s), except 1.9% for the film surface (0 s). The Si element was

TABLE III
Elemental Composition of PIS*x*-*y*-*z*T Hybrid Films Under Depth Profiling

Samples	Depth profile time (s)	Composition[1] (atomic percentage, %)				
		C 1s	O 1s	N 1s	Si 2p	Ti 2p
PIS0-00-4T	0	80.0	14.3	3.0	1.9	0.7
	30	91.2	3.9	2.2	0	2.7
	60	91.5	3.6	3.3	0	3.0
	90	91.1	3.3	2.0	0	3.6
	120	90.2	4.1	2.0	0	3.6
PIS6-10-0T	0	70.2	17.1	2.0	10.7	0
	30	85.3	5.2	2.3	7.1	0
	60	87.3	5.3	2.3	5.1	0
	90	88.9	4.2	2.1	4.7	0
	120	89.6	3.7	2.3	4.4	0
PIS6-10-4T	0	70.9	19.3	3.2	5.1	1.6
	30	75.5	16.2	3.4	3.0	2.0
	60	77.6	14.6	3.2	2.5	2.2
	90	78.8	13.6	3.3	2.1	2.2
	120	79.5	13.3	3.0	1.8	2.3

[1] Determined by relative intensity of characteristic peaks from XPS spectra.

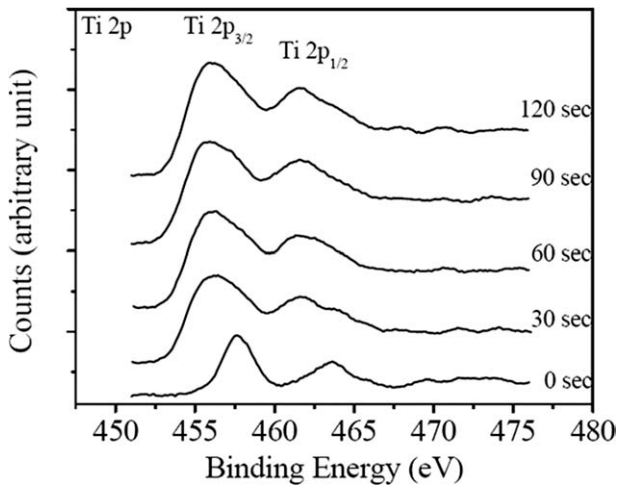

Figure 6 XPS (Ti 2p) spectra of PIS0-00-4T hybrid films under depth profiling (0 to 120 s).

only distributed on the surface for hybrid films without the presence of APPS or TiO_2. The distribution of Ti element was different from that of Si. Figure 6 demonstrated Ti binding energy of PIS0-00-4T under depth profiling. On the top surface of PIS0-00-4T, i.e., 0-s curve, the binding energy of Ti $2p_{3/2}$ and Ti $2p_{1/2}$, which was 457.8 and 463.7 eV, respectively, indicated the presence of TiO_2.[30–32] A longer sputtering time was associated with higher peak intensity. Accordingly, the Ti content in the bulk exceeded that on the surface of PI. In the contrary, there was more Si on the surface. The Ti binding energy shifted toward a lower value for samples under sputtering. The Ti binding energy of $2p_{3/2}$ and Ti $2p_{1/2}$ was 455.8 and 461.7 eV, respectively, for samples under 120-s sputtering. With the increase in film depth, the oxygen content may not be sufficient to completely convert titanium alkoxide into TiO_2.[1]

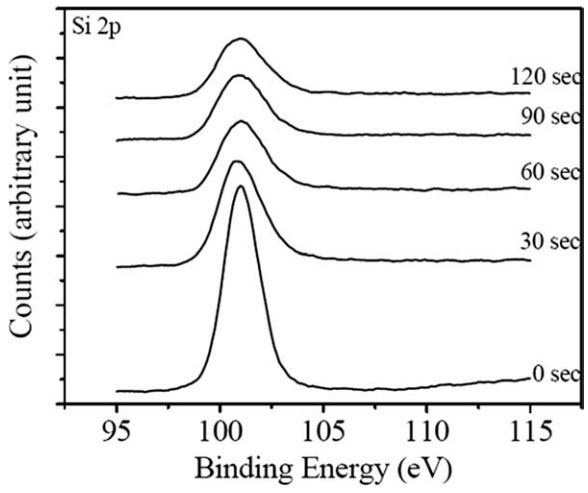

Figure 7 XPS (Si 2p) spectra of PIS6-10-0T hybrid films under depth profiling (0 to 120 s).

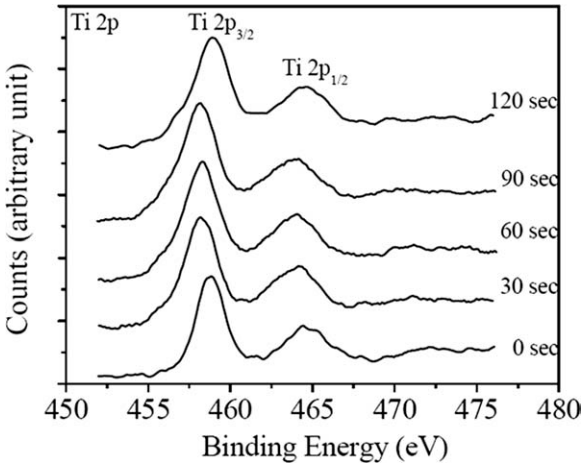

Figure 8 XPS (Ti 2p) spectra of PIS6-10-4T hybrid films under depth profiling (0 to 120 s).

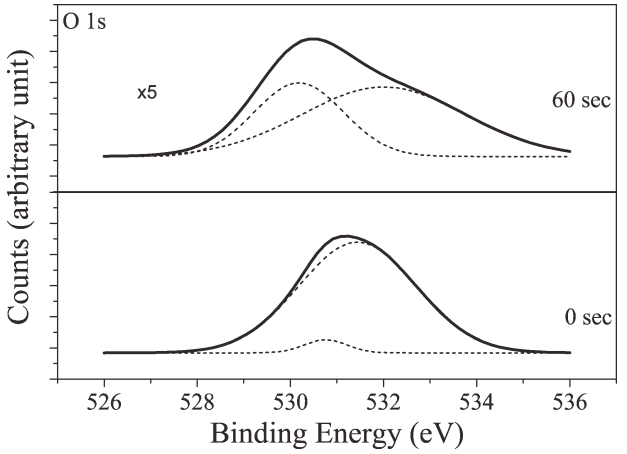

Figure 10 XPS (O1s) spectra (solid lines) and deconvolution results (dash lines) of PIS0-00-4T hybrid films under depth profiling (0 and 60 s). The scale of *y*-axis of 60-s curves is 5-time of 0-s curves.

The XPS (Si 2p) depth profile of PIS6-10-0T was shown in Figure 7. The intensity of Si-C peak at 100.9 eV[33] decreased remarkably with the increase of the sputtering time. The Si composition of PIS6-10-0T shown in Table III also revealed higher Si content on the surface than in the bulk. The result was consistent with Jwo et al.[9] that silicon tends to distribute on the surface rather than in the bulk. Contrarily, Ti tends to distribute inside the PIS0-00-4T film.

Figure 8 presented the XPS (Ti 2p) spectra of PIS6-10-4T and Table III listed the details of each composition. The Ti content on the surface of PIS6-10-4T was 1.6%, which significantly exceeded that of PIS0-00-4T (0.7%). Most of the Ti elements in PIS0-00-4T were more homogeneously dispersed inside revealing similar peak intensity for samples under various sputtering time (Fig. 6). With the presence of APPS, the Ti binding energies of PIS6-10-4T (0-s), 458.8 and 464.5 eV, were larger than those of PIS0-00-4T, 457.8 and 463.7 eV, respectively. This shift was consistent with that observed by other groups.[34–36] Moreover, the shift of Ti (2p) binding energy in PIS6-10-4T at various depths was less significant than that in PIS0-00-4T.

The XPS (Si) spectra of PIS6-10-4T shown in Figure 9 were compared with the ones of PIS6-10-0T (Fig. 7). The Si content for PIS6-10-4T decreased notably with the increasing sputtering time, similar to the result of PIS6-10-0T. The effect of depth on Si composition can also be revealed from Table III. The position of main Si peak, corresponding to Si—C, for the top surface of PIS6-10-4T was around 102.0 eV, which was higher than that of PIS6-10-0T, 100.9 eV. Without the presence of TiO_2, the position of Si—C peak remained unchanged under depth profiling. In this study, the TiO_2 network may be arranged by breaking the Si—O—Si chain of the APPS

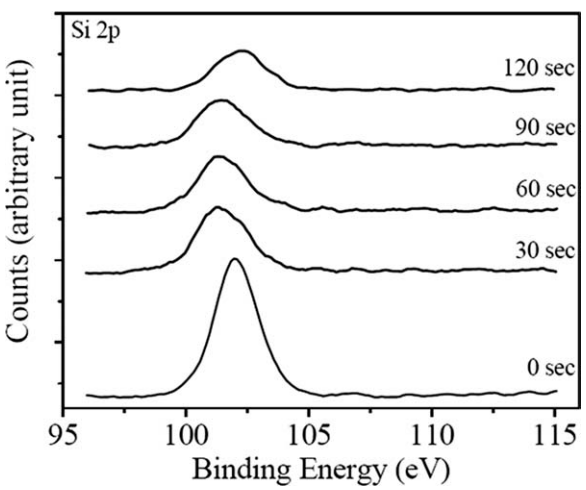

Figure 9 XPS (Si 2p) spectra of PIS6-10-4T hybrid films under depth profiling (0 to 120 s).

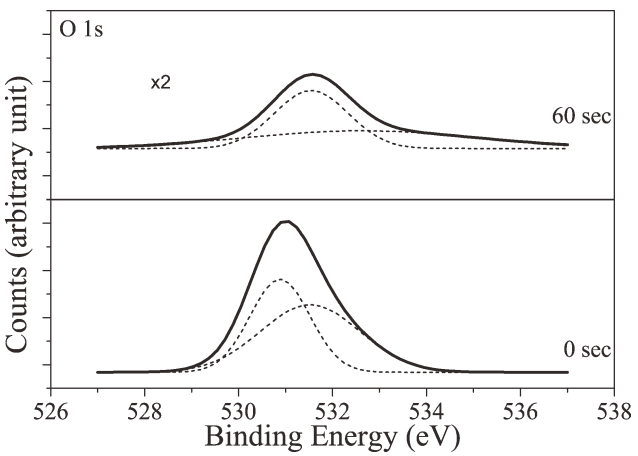

Figure 11 XPS (O1s) spectra (solid lines) and deconvolution results (dash lines) of PIS6-10-0T hybrid films under depth profiling (0 and 60 s). The scale of *y*-axis of 60-s curves is two-time of 0-s curves.

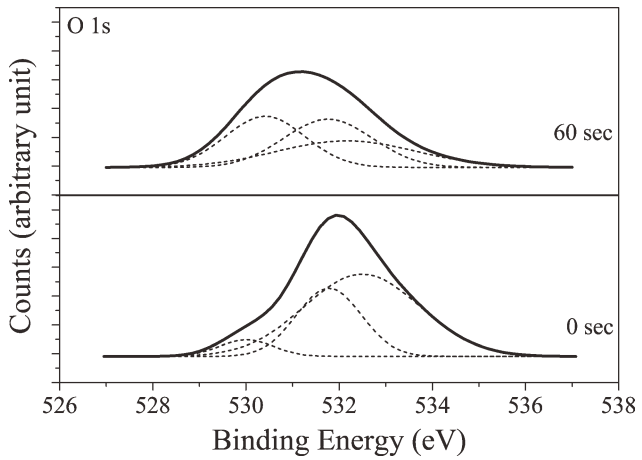

Figure 12 XPS (O1s) spectra (solid lines) and deconvolution results (dash lines) of PIS6-10-4T hybrid films under depth profiling (0 and 60 s).

composition or bonding between both Si and Ti with the C=O group in PIS.[35] Those Ti elements in the inner layer were then pulled to the surface by Si, which has a high surface energy and therefore caused more Ti presenting on the surface of PIS6-10-4T than that of PIS0-00-4T, which does not contain APPS.

The XPS (O 1s) spectra for samples (PIS0-00-4T, PIS6-10-0T, and PIS6-10-4T) under 0-s and 60-s depth profiling as well as the Gaussian deconvolution of overlapped peaks were shown in Figures 10–12. From Figure 10, the overlapped oxygen peak of the surface of PIS0-00-4T (0 s) was attributed to the following components, SiO_xN_y or SiO_2 (530.8 eV) and C=O (531.5 eV), respectively.[34–37] Based on previous sections, the surface of PIS0-00-4T had less Ti than Si. Consequently, the oxygen (1s) peak shown in Figure 10 was considered as Si-related oxides rather than Ti—O components. Sputtering for 60 s completely eliminates the peak of Si-related oxides (530.8 eV) that the new deconvolution results, believed to be Ti—O[36,38,39] and C=O, were obtained at 530.0 and 532.0 eV, respectively.

TABLE IV
Peel Strength of PIS6-10-zT Hybrid Films

Samples	Peel strength (N cm^{-1})[1]
PIS6-10-0T	5.82
PIS6-10-1T	6.58
PIS6-10-2T	6.96
PIS6-10-4T	3.06
PIS0-00-4T	–[2]

[1] Averages of four measurements.
[2] The hybrid film is too brittle and fragile to obtain satisfactory measurement.

In Figure 11, the surface of PIS6-10-0T showed two overlapping XPS (O1s) peaks, corresponding to SiO_xN_y or SiO_2 (530.8 eV) and C=O (531.5 eV). The relative intensity of the SiO_xN_y or SiO_2 peak from PIS6-10-0T was much stronger than that from PIS0-00-4T (Fig. 10). Sputtering for 60 s clearly led to the appearance of another two overlapping peaks, C=O (531.5 eV) and Si—O—Si (532.6 eV).[28] No detectable Si—O—Si peak was observed from the surface of PIS6-10-0T. Si content was higher on the surface than in the bulk, which was consistent with result shown in Figure 7.

Figure 12 showed three overlapping oxygen (1s) peaks, which corresponded to TiO_2 (529.9 eV), C=O (531.7 eV), and Si—O—Si (532.5 eV), respectively, from the surface of PIS6-10-4T. With the increase of sputtering time, the relative peak intensity of TiO_2 increased and was accompanied by the decrease in intensity of Si—O—Si peak. Moreover, a shifting of C=O binding energy was observed from Figures 10–12. Hybrid films containing TiO_2 (Figs. 10 and 12) showed higher C=O binding energy than TiO_2-abscent films (Fig. 11) do. The presence of elemental Ti may react with C=O groups in PIS to form Ti—O.

Peel strength test

The adhesive strength between PIS6-10-*z*T hybrid film and copper foil was presented in Table IV. The peel strength of those hybrids increased with TiO_2 content up to 2 wt %. A reduce in peel strength was observed for PIS6-10-4T, which contained 4 wt % of TiO_2. Similar phenomenon had been reported by Chiang et al.[23] that further adding of TiO_2 in PI significantly reduces the peel strength of TiO_2/PI-copper system. The films with high content of TiO_2 (>4 wt %) were brittle that fracture happened during

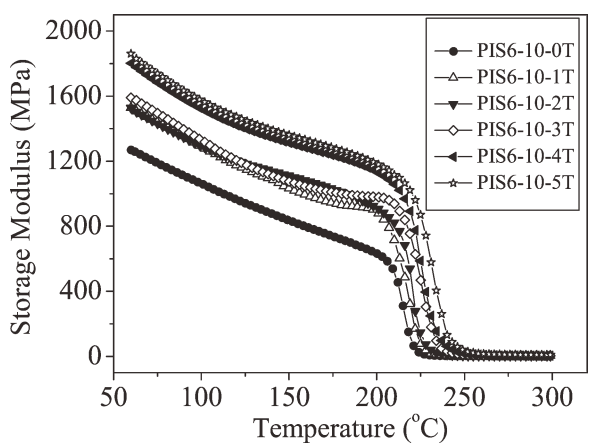

Figure 13 Storage modulus of poly(imide siloxane) (PIS) and PIS/TiO_2 hybrid films.

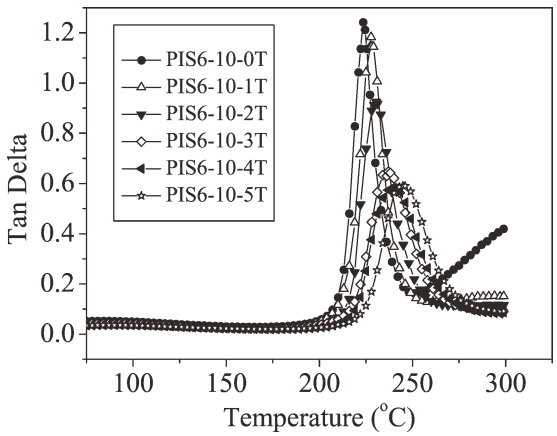

Figure 14 Tan delta curves of poly(imide siloxane) (PIS) and PIS/TiO_2 hybrid films.

peel strength measurements. In this study, the peel strength of the hybrids with 1 and 2 wt % TiO_2 exceeded that of PIS6-10-0T (without TiO_2). The increase in peel strength was probably because some of the TiO_2 was pulled to the surface to increase the strength of the adhesion between the hybrids and the copper foil.

Dynamic mechanical analysis

The dynamic mechanical properties of PIS/TiO_2 hybrid films as a function of temperature were shown in Figures 13 and 14. Figure 13 shows the storage modulus of PIS/TiO_2 hybrid films. The storage modulus of hybrid films was enhanced when the content of TiO_2 within films was increased. For all the PIS/TiO_2 hybrid films, their glass transition temperature (T_g) were assigned at each maximum of tan δ curves in Figure 14. Same increasing trend was observed for the T_g of the hybrid films, from 224 to 246°C, when the content of TiO_2 was increased from 0 to 5 wt %. Similar results were observed from the studies of Liaw et al.[40] This result could be attributed to the filler effect of TiO_2, thereby affording stiffer hybrid films. Besides, the crosslinking reaction occurred between PIS and $Ti(OEt)_4$ is also expected to increase the T_g value.

CONCLUSIONS

Titanium oxides were successfully introduced into the PIS membrane. Thermal analysis demonstrated that the CTE value of PIS6-10-1T was halved of the one of PIS6-10-0T. The CTE decreased significantly with the increase in TiO_2 content in hybrids, while the decomposition temperature (T_d) slightly decreased. The Si concentration on surface was much higher than that in the bulk of hybrids, while Ti tended to distribute in the bulk. On the other hand, the presence of APPS can promote the formation of TiO_2 on the surface. The interaction between APPS and TiO_2 on the surface, in turn, affected the surface characteristics and adhesion of PIS/TiO_2 films. Adding 1 or 2 wt % TiO_2 into hybrids effectively improved the peel strength of hybrids copper system. When the TiO_2 content increased over 4 wt %, the films became too stiff and brittle to examine the peel strength.

References

1. Chiang, P. C.; Whang, W. T. Polymer 2003, 44, 2249.
2. Ghosh, M. K.; Mittal, K. L. Polyimides: Fundamentals; Applications; Marcel Dekker: New York, 1996.
3. Mittal, K. L. Polyimides: Synthesis, Characterization,; Applications; Plenum Press: New York, 1984.
4. Nakamura, Y.; Suzuki, Y.; Watanabe, Y. Thin Solid Films 1996, 290, 367.
5. Ektessabi, A. M.; Hakamata, S. Thin Solid Films 2000, 621, 377.
6. Okugawa, Y.; Yoshida, T.; Suzuki, T.; Nakayoshi, H. IEEE 1994, 570.
7. Tsai, M. H.; Whang, W. T. Polymer 2001, 42, 4197.
8. Jwo, S. L.; Whang, W. T.; Liaw, W. C. J Appl Polym Sci 1999, 74, 2832.
9. Jwo, S. L.; Whang, W. T.; Hsieh, T. E.; Pan, F. M.; Liaw, W. C. J Polym Res 1999, 6, 175.
10. Tasi, M. H.; Chiang, P. C.; Whang, W. T.; Ko, C. J.; Huang, S. L. Surf Coat Tech 2006, 200, 3297.
11. Ku, C. K.; Ho, C. H.; Chen, T. S.; Lee, Y. D. J Appl Polym Sci 2007, 104, 2561.
12. Matienzo, L. J.; Egitto, F. D. J Mater Sci 2007, 42, 239.
13. Kondoh, E. Thin Solid Films 2000, 359, 255.
14. Ohuchi, F. S.; Freilich, S. C. J Vac Sci Technol 1986, A4, 1039.
15. Hu, C. J.; He, Z. H.; Fu, W. C.; Qi, Z. J Phys D: Appl Phys 2009, 42, 185303.
16. Byun, T. J.; Kim, S. I.; Kim, Y. J.; Choi, Y. S.; Choi, I. S.; Setsuhara, Y.; Han, J. G. Jpn J Appl Phys 2009, 48, 08HL01.
17. Murugaraj, P.; Mainwaring, D. E.; Chen, L. G.; Sawant, P.; Kobaisi, M. A.; Yek, W. M. J Appl Polym Sci 2010, 115, 1054.
18. Chou, N. J.; Tang, C. H. J Vac Sci Technol 1984, A2, 751.
19. Borris, J.; Dohse, A.; Hinze, A.; Thomas, M.; Klages, C. P.; Möbius, A.; Elbick, D. Weidlich, E. R. Plasma Process Polym 2009, 6, S258.
20. Uemura, A.; Kezuka, K.; Iwamori, S.; Nishiyama, I. Vacuum 2010, 84, 607.
21. Joo, S.; Baldwin, D. F. Nanotechnology 2010, 21, 55204.
22. Tsai, M. H.; Ko, C. J. Surf Coat Tech 2006, 201, 4367.
23. Chiang, P. C.; Whang, W. T.; Wu, S. C.; Chung, K. R. Polymer 2004, 45, 4465.
24. Andolino Brandt, P. J.; Senger Elsbernd, C. L.; Patel, N.; York, G.; McGrath, J. E. Polymer 1990, 31, 180.
25. Tasi, M. H.; Whang, W. T. J Appl Polym Sci 2001, 81, 2500.
26. Summers, J. D. Ph. D. Dissertation: Siloxane Modified Engineering Polymer: Synthesis; Characteristics, Virginia Polytechnic Institute; State University, Blacksburg, VA, 1988.
27. Liu, L.; Lu, Q.; Qian, X.; Wang, W.; Zhu, Z.; Wang, Z. Mater Chem Phys 2002, 74, 210.
28. Hu, Q.; Marand, E. Polymer 1999, 40, 4833.
29. Sawada, T.; Ando, S. Chem Mater 1998, 10, 3368.
30. Boggess, R. K.; Taylor, L. T. J Polym Sci Polym Chem Ed 1987, 25, 685.
31. Rancourt, J. D.; Taylor, L. T. Macromolecules 1987, 20, 790.

32. Jouan, P. Y.; Peignon, M. C.; Cardinaud, C.; Lemperiere, G. Appl Surf Sci 1993, 68, 595.
33. Hamrin, K.; Johansson, G.; Fahlman, A.; Nordling, C. J Phys Chem Solids 1969, 30, 1835.
34. Keshavaraja, A.; Ramaswamy, V.; Soni, H. S.; Ramaswamy, A. V.; Ratnasamy, P. J Catal 1995, 157, 501.
35. Contarini, S.; Howlett, S. P.; Rizzo, C.; De Angelis, B. A. Appl Surf Sci 1991, 51, 177.
36. Jung, S. M.; Dupont, O.; Grange, P. Appl Catal A-Gen 2001, 208, 393.
37. Lee, W. J.; Lee, Y. S.; Rha, S. K.; Lee, Y. J.; Lim, K. Y.; Chung, Y. D.; Whang, C. N. Appl Surf Sci 2003, 205, 128.
38. Bertoti, I.; Varsanyi, G.; Mink, G.; Szekely, T.; Vaivads, J.; Millers, T.; Grabis, J. Surf Interface Anal 1988, 12, 527.
39. Gardner, S. D.; Singamsetty, S. K. C.; Booth, G. L.; He, G. R. Carbon 1995, 33, 587.
40. Liaw, W. C.; Chen, K.P. Eur Polym J 2007, 43, 2265.